RAPID COMMUNICATIONS

PHYSICAL REVIEW B VOLUME 44, NUMBER 7 15 AUGUST 1991-I

Large lattice-relaxation-induced electronic level shifts in random $Cu_{1-x}Pd_x$ alloys

Z. W. Lu, S.-H. Wei, and Alex Zunger
Solar Energy Research Institute, Golden, Colorado 80401
(Received 20 May 1991)

Mean-field theories of unrelaxed $Cu_{0.75}Pd_{0.25}$ alloys exhibit a deep ($\varepsilon_F - 5.5$ eV) Pd bonding state at the bottom of the Cu d band that does not show up in photoemission experiments. We have applied the "special quasirandom structures" construct to $Cu_{1-x}Pd_x$ alloys in the context of local-density total-energy minimization, finding a *distribution* of Cu–Cu, Cu–Pd, and Pd–Pd bonds whose lengths deviate significantly from the single, unrelaxed value assumed in mean-field models. Such lattice distortions are found to induce a $\sim$ 1-eV shift in the Pd bonding state to lower binding energies, thus removing much of the discrepancy with experiment.

Electronic-structure calculations[1–11] on transition-metal (TM) impurities in noble metals and on the corresponding alloy systems often show two impurity-induced peaks in the density of states (DOS), lying, respectively, near the top and the bottom of the host crystal d band. While the higher state near the Fermi energy ε_F is clearly apparent in many calculations[1–11] and in photoemission experiments,[12–17] theoretical characterization and experimental identification of the deep state near the bottom of the d band remains elusive. It is seen in calculations for Cu-Pd,[1,3–8] but not in Cu-Ni (Ref. 3) or Ag-Pd.[3] Since the energy and amplitude of the state at the bottom of the d band represents a balance between different bonding effects in TM intermetallics, understanding its origins has become a central issue in this field, as perhaps best exemplified by the many theoretical[1–11] and experimental[12–17] studies of this state in Cu-Pd.

While coherent-potential-approximation (CPA) calculations of $Cu_{0.75}Pd_{0.25}$ [using the Korringa-Kohn-Rostoker (KKR) method] exhibit the deep lying state at $\varepsilon_F - 5.5$ eV,[1,3–7] photoemission[12–16] and Auger[17] experiments did not observe this deep state. These calculations[3–8] have identified the nature of the impurity-induced states: the two peaks are associated with bonding and antibonding states formed from the impurity d level that are coupled to the surrounding host atoms. If the impurity atom has a deeper d orbital energy than the host atom (e.g., *Cu*:Au), it will create a deep, impurity-like state that broadens into an "impurity band" at high concentrations[2,3] ("split-band alloy"). Depending on the proximity between the impurity and host d energy levels, weakly hybridized states will also appear near the host d bands. On the other hand, if the impurity d orbital energies are close to the host d bands (e.g., *Cu*:Pd) hybridization and level repulsion will create a pair of mutually repelled and highly mixed bonding-antibonding states plus a "vacancylike" band that is located at the intermediate energies.[1,3] At high impurity concentration this leads to a "common-band alloy."

This analysis[3,18] identifies the factors controlling the position of the deep state: since for Cu-Pd this state is both "impuritylike" and "bonding," a reduction in the attractiveness of the Pd potential will displace this state to lower binding energy, as will an *increase* in the Cu–Pd and Pd–Pd bond lengths (since bonding states are destabilized by an increase in the bond length[18]). These factors were recognized by van der Marel, Jullianus, and Sawatzky[15] and by Stefanou *et al.*[9] in the context of the dilute impurity limit. The latter authors have demonstrated that increasing (arbitrarily) the impurity-host bond length led to a shift in the bonding state to lower binding energies, thus improving the agreement with experiment. Generalization of these ideas to the concentrated alloy limit[10,11] proved, however, difficult. While in the dilute impurity case there is but a *single* local environment about the impurity (coordinated by 12 host atoms), the $A_{1-x}B_x$ alloy manifests a *distribution* of local environments (e.g., A coordinated by the various A_mB_{12-m} clusters with $0 \le m \le 12$), each having distinct bond lengths and effective charge.[19] Many of the currently available alloy theories (e.g., the CPA, Refs. 3–8) invoke at the outset a mean-field description, whereby all A atoms (and separately, all B atoms) are taken to be crystallographically equivalent, so symmetry-lowering relaxations and environmental effects on charges[19] are not considered. While in the $L1_2$ ordered Cu_3Pd compound all Cu–Cu, Pd–Pd, and Cu–Pd bond lengths are equal by symmetry, it is not obvious that the *disordered* alloy is at its lowest energy state when all bonds have equal lengths,[3–8] or whether there is a *single value* to the e.g., Cu–Cu bond length.

These questions can be tested by considering a *structural* model for the alloy. This is possible, for example, using the "special quasirandom structures" (SQS) construct,[20] where one applies band-structure techniques to a repeated supercell whose sites are occupied by A and B atoms so as to reproduce, by design, the average many-body correlation functions of a perfectly random infinite alloy. Hence, instead of requiring[3–8] that *each* atom be influenced by an identical, average medium, we create a *distribution* of distinct environments whose average corresponds to the random medium. The geometric inequiv-

alence of the various A sites can hence derive concomitant fluctuations in the charge distribution on different A sites and bond lengths.[21,22]

The $x = \frac{1}{2}$ alloy is described through the SQS-$\frac{1}{2}$ supercell considered previously;[20–22] this structure can be described as an $A_1B_2A_3B_2$ superlattice along the [113] direction. The $x = \frac{1}{4}$ (or $x = \frac{3}{4}$) alloy is described by the SQS-$\frac{1}{4}$ supercell consisting of A_6B_2 layers stacked along the [201] direction. The electronic structure of the SQS's is calculated using the general potential semirelativistic linearized augmented plane-wave (LAPW) method[23] with Wigner exchange correlation. A basis set consisting of $\sim$ 100 (85) LAPW's are used for SQS-$\frac{1}{2}$ (SQS-$\frac{1}{4}$), corresponding to kinetic energy cutoff of 16.7 Ry. During the self-consistency iterations (and subsequent total-energy evaluations), the Brillouin-zone summation were carried out using 128 (96) special $\mathbf{k}$ points for SQS-$\frac{1}{2}$ (SQS-$\frac{1}{4}$). The DOS are then calculated using the tetrahedron integration method[24] using eigenvalues at 117 (93) $\mathbf{k}$ vectors in the irreducible zone. The resulting DOS were smoothed using a Gaussian function with a full width at half maximum of 0.2 eV.

Total-energy minimization is first applied to fcc and bcc Cu and Pd, finding the equilibrium fcc lattice parameters 3.562 and 3.882 Å, respectively. An analogous calculation for CuPd in $B2$ (CsCl) structure showed that the equilibrium volume is within 0.5% of the linear-weighted values of its bcc constituents; we hence apply this linear description (Vegard's rule) to the alloy.

Figure 1(a) shows the radially displaced electronic charge density $\Delta\rho(\mathbf{r}) = 4\pi r^2[\rho(\mathbf{r}) - \rho_{\rm fcc}(\mathbf{r})]$ for various *ordered* CuPd compounds relative to the pure fcc metal of the same volume. The overall direction of charge transfer upon compound formation is seen to be from the high-density Pd metal to the low-density Cu metal, consistent with the relative core chemical shifts seen[12–14] in photoemission studies. Different ordered structures are distinguished by the number of like atoms around a given site (integers shown in Fig. 1). We see from Fig. 1(a) that *the magnitude of charge transfer is proportional (in fact, linearly) to the number of unlike atoms in the first coordinate shell.* Hence, crystallographically inequivalent A atoms have different charges. Figure 1(b) shows the displaced charge in the random $Cu_{0.5}Pd_{0.5}$ alloy modeled by the SQS, exhibiting precisely the same trend: chemically identical but crystallographically inequivalent sites have different degrees of charge transfer, e.g., $Cu^{(2)}$ (coordinated by 2Cu+10Pd) gains more charge than the $Cu^{(8)}$ (coordinated by 8Cu+4Pd). The existence of a *distribution* of charges for the same type of atoms lowers[19] the electrostatic lattice energy and (along with the concomitant fluctuations in atomic sizes) can drive lattice relaxation. We next investigate its effect on the alloys electronic structure.

The relaxed geometry of the alloy is determined from first-principles total-energy calculations on the respective SQS's at given volume $V(x)$. While straightforward, the large number of cell-internal structural degrees of freedom make this calculation computer intensive, hence, there is a premium on finding a reasonable initial guess. This can be done by realizing that the SQS's can also be

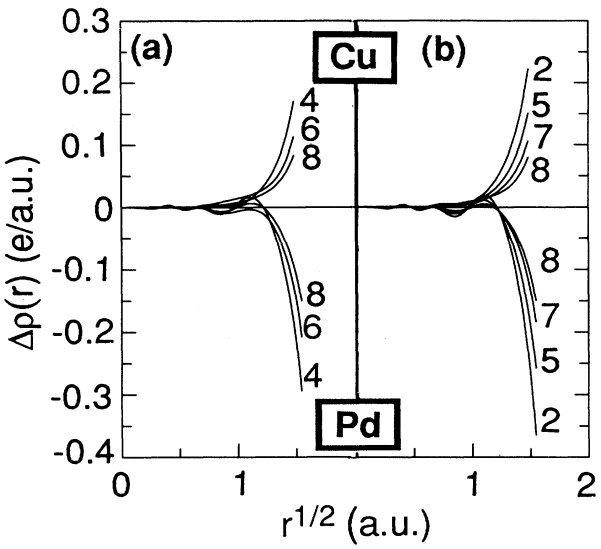

FIG. 1. Difference between the radial charge density of intermetallic CuPd systems and that of its elemental fcc constituents at the same lattice constants. Integers denote the number N of like atoms in the first coordination shell. (a) Ordered compounds, $N = 4$ is $L1_0$, $N = 6$ is $L1_1$, and $N = 8$ is the Cu_2Pd_2 (001) superlattice. (b) the random SQS alloy at the same composition, showing a distribution of N's. Note that in both cases the charge transfer is proportional to $12 - N$. The muffin-tin radii are $R_{\rm MT}^{\rm Cu}$= 2.2 a.u. and $R_{\rm MT}^{\rm Pd}$= 2.4 a.u.

described as "superlattices" along some special orientations $\mathbf{G}$= $[l, m, n]$, and that continuum elasticity theory[25] provides the equilibrium interlayer spacing along $\mathbf{G}$ as a function of the externally-fixed perpendicular lattice constant $a_\perp$ as

$$c_{\rm eq}^{(\lambda)}(a_\perp) = a_{\rm eq}^{(\lambda)} - [2 - 3q_\lambda(\mathbf{G})][a_\perp - a_{\rm eq}^{(\lambda)}] , \qquad (1)$$

where $a_{\rm eq}^{(\lambda)}$ is the equilibrium cubic lattice constant of material λ. Here, $q_\lambda(\mathbf{G})$ is the "strain reduction factor" along $\mathbf{G}$ given by[25] $q(\mathbf{G}) = 1 - B/[C_{11} + \gamma(\mathbf{G})\Delta]$, where $\Delta = C_{44} - (C_{11} - C_{12})/2$ is the elastic anisotropy, B is the bulk modulus, C_{ij} are the elastic constants, and the orientation dependence is given by the geometric constant

$$\gamma(\mathbf{G}) = \frac{4(l^2m^2 + m^2n^2 + n^2l^2)}{(l^2 + m^2 + n^2)^2} , \qquad (2)$$

e.g., $\gamma(001) = 0$, $\gamma(201) = \frac{16}{25}$, and $\gamma(113) = \frac{76}{121}$. While the elemental solids Cu and Pd have the equilibrium lattice constants $a_{\rm eq}^{(\lambda)}$, in the alloy environment these will expand and contract, respectively, to the alloy value $a_\perp = a(x)$. We then imagine a coherent layer of pure Cu (or Pd) whose lattice constant $\alpha_\perp$ perpendicular to $\mathbf{G}$ is constrained to equal $a(x)$, finding from Eqs. (1) and (2) the Cu–Cu (or Pd–Pd) interlayer distances along $\mathbf{G}$. We then layer these Cu and Pd planes in the SQS, finding the corresponding Cu and Pd atomic position so that the interlayer distances matches those obtained above. To examine the accuracy of this relaxation model, we first

TABLE I. Comparison of the tetragonal deformation $c_{eq}(a_\perp)/a_\perp$ for the $L1_0$ structure of the CuPd as calculated for a range of perpendicular lattice constants $a_\perp$ by the LAPW method and from the continuum elasticity [Eq. (1), $c_{eq} = \frac{1}{2}(c_{eq}^{Cu} + c_{eq}^{Pd})$].

$a_\perp$ (Å)	$c_{eq}/a_\perp$ LAPW	$c_{eq}/a_\perp$ Eq. (1)	% error
3.662	1.046	1.044	0.2
3.739	0.988	0.992	0.4
3.803	0.947	0.949	0.2
3.872	0.903	0.905	0.2

test it on CuPd in the $L1_0$ structure (a [001] superlattice), where accurate LAPW energy minimization is easily performed. We compare the tetragonal deformation calculated from Eqs. (1) and (2) for a series of externally fixed $a_\perp$ values, with those obtained from direct LAPW total-energy minimizations. Table I shows that the elastic model is remarkably accurate over a wide range of deformations. We have next applied this elastic model to the SQS, obtaining an initial guess for the relaxed atomic positions. This is then refined by minimizing the LAPW total energy with respect to all atomic positions. This is done by calculating the quantum-mechanical forces using the method of Yu, Singh, and Krakauer.[26] We find that the fully relaxed geometry is rather close to that predicted by the elastic model: the average bond lengths changed by less than 0.5% and the total energy was reduced by less than 2 meV/atom. We find that the mixing enthalpy of the disordered alloy $\Delta H_{mix}(x)$ was reduced from the fully unrelaxed value of -45.0 meV/atom at $x = \frac{1}{2}$ to the fully relaxed value of -62.5 meV/atom; for $x = \frac{1}{4}$ the reduction is from -28.6 meV/atom to -50.3 meV/atom. Clearly, atomic relaxations (absent by symmetry in the ordered $L1_2$ Cu_3Pd compound and neglected in previous CPA alloy calculations) are very significant in the disordered $Cu_{1-x}Pd_x$ alloy. Note that not only does this atomic relaxation produce three types of bonds with distinct lengths (Cu–Cu, Cu–Pd, and Pd–Pd) but that this also creates a *distribution* of different lengths for each of these bond types at a given x. Analogous LAPW calculations for the ordered $B2$ structure give $\Delta H = -97.6 < \Delta H_{mix}(1/2)$, hence $B2$ ordering at low temperature can be expected.

Figure 2 displays the calculated bond lengths in $Cu_{1-x}Pd_x$ (each averaged, for convenience of display over its distribution whose widths is denoted in the caption). Three features are noteworthy: (i)All bond lengths deviate both from the "ideal" values in the pure constituents assumed in the calculation of Refs. 10 and 11; they also deviate from the common "virtual lattice" values $R = (\sqrt{2}/2)[(1-x)a_{Cu} + xa_{Pd}]$ (dotted diagonal line), assumed in all CPA calculations.[3–8] (ii) The *width* (~ 0.05 Å) of the distribution for each bond type in $Cu_{1-x}Pd_x$ is comparable to the difference in the average bond lengths, e.g., the difference $\langle R_{Pd\text{-}Pd}\rangle - \langle R_{Cu\text{-}Cu}\rangle$ is 0.078, 0.073, and 0.069 Å at $x = \frac{1}{4}$, $\frac{1}{2}$, and $\frac{3}{4}$, respectively. (iii) The bond lengths in the random alloy are significantly different from those in the ordered $L1_0$ or $L1_2$ compounds at

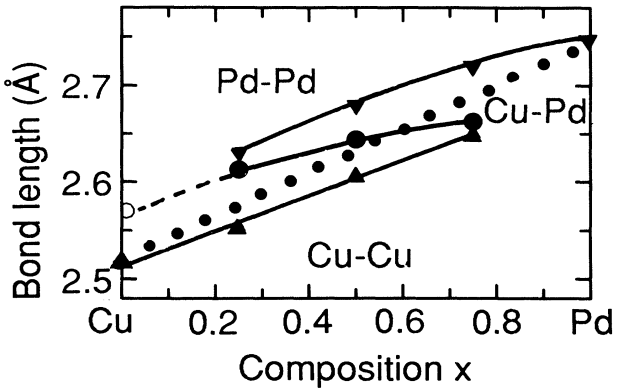

FIG. 2. Average bond lengths in $Cu_{1-x}Pd_x$. The diagonal dotted line gives the virtual lattice average used in Refs. 3–8. Calculated points (joined by lines to guide the eye) represent the average over distributions whose standard deviations are 0.052 and 0.050 Å for Pd-Pd at $x = \frac{1}{4}$ and $x = \frac{1}{2}$ and 0.052 and 0.063 Å for Cu-Pd at the same compositions. The open circle denotes the extrapolated Cu–Pd bond length for dilute $Cu_{0.99}Pd_{0.01}$ alloy. It is found to be 2% larger than the Cu-Cu distance in pure Cu.

the same composition x_c [e.g., at $x = \frac{1}{4}$ the bond lengths for the $L1_2$ structure are $\sqrt{2}/2a(x)$] in contrast with the assumption underlying the calculations of Refs. 6 and 7; the similarities found there in the DOS's of ordered and disordered systems could, in part reflect the assumption

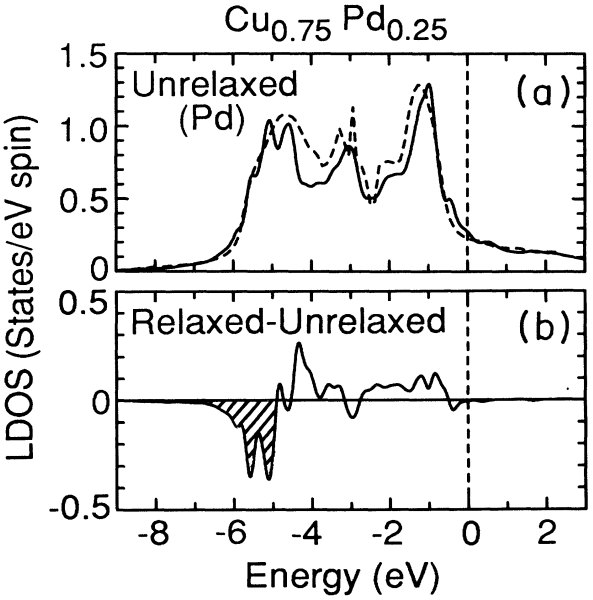

FIG. 3. (a) Density of states of Pd inside the muffin-tin spheres in the $Cu_{0.75}Pd_{0.25}$ unrelaxed geometry. The solid line is the present LAPW result ($R_{MT}^{Pd} = 2.4$ a.u.), while the dashed line is the previous KKR-CPA result. (b) The DOS difference between the relaxed and unrelaxed geometries as calculated by the LAPW method.

of equal bond lengths in the two phases.

We fitted the calculated Cu–Pd bond lengths at $x = \frac{1}{4}$, $\frac{1}{2}$, and $\frac{3}{4}$ to a parabolic function. By extrapolating the result to the dilute limit $x = 0$, we found that there is a lattice expansion of 2.0% around a Pd impurity (open circle in Fig. 2), in good agreement with the extended x-ray absorption fine-structure (EXAFS) experiment showing[27] a 2% expansion.

The top part of Fig. 3 compares the Pd local DOS in the unrelaxed SQS for $Cu_{0.75}Pd_{0.25}$ with the unrelaxed KKR-CPA results of Ginatempo *et al.*:[7] There is an overall agreement (except that the broad single structure centered around $\varepsilon_F - 5$ eV is split in our calculation into a doublet).

The effect of relaxation on the Pd local DOS is illustrated in the bottom part of Fig. 3, displaying the difference between our relaxed and unrelaxed results. The *increase* in the Cu–Pd and Pd–Pd bond lengths over their common virtual lattice values (Fig. 2) removes intensity in the density of states from the bottom of the band at $\sim \varepsilon_F - 5.5$ eV, resulting in much better agreement with experiment.[16] Interestingly, the effect of relaxation on the Cu LDOS is negligible; the more tightly bound (and narrower) Cu d states are less responsive to bond deformations. This is also evidenced by the fact that DOS of pure fcc Cu shifts by less than 0.3 eV when the cubic lattice parameter is changed from the values of 3.646 Å(approximate to the alloy at $x = \frac{1}{4}$) to 3.739 Å (approximate to the alloy at $x = \frac{1}{2}$). The change in the DOS of pure Pd under the same deformation is much larger (0.7 eV).

We conclude that unlike the ordered $L1_2$ phase, the random alloy has a distribution of bond lengths and charges (neglected in current mean-field theories) and that atomic relaxations expand the long bond (e.g., Pd–Pd in CuPd). This results in a substantial shift of the bonding state to lower binding energies ($\sim$ 1 eV in $Cu_{0.75}Pd_{0.25}$) therefore removing much of the discrepancy with experiment.

We are grateful to Dr. R. Yu and Dr. D. Singh, and Professor H. Krakauer for providing us with the LAPW force program and to Dr. B. Ginatempo for providing the LDOS of Pd (Ref. 7) for comparison. This work was supported by the Office of Energy Research (OER) [Division of Materials Science of the Office of Basic Energy Science (BES)], U.S. Department of Energy, under Contract No. DE-AC02-77-CH00178.

[1] P. J. Braspenning, R. Zeller, P. H. Dederichs, and A. Lodder, J. Phys. F **12**, 105 (1982); P. J. Braspenning, R. Zeller, A. Lodder, and P. H. Dederichs, Phys. Rev. B **29**, 703 (1984).
[2] V. L. Moruzzi, A. R. Williams, and J. F. Janak, Phys. Rev. B **10**, 4856 (1974).
[3] R. S. Rao, A. Bansil, H. Asonen, and M. Pessa, Phys. Rev. B **29**, 1713 (1984).
[4] J. Kudrnovsky and J. Masek, Phys. Rev. B **31**, 6424 (1985).
[5] H. Winter, P. J. Furham, W. M. Temmerman, and G. M. Stocks, Phys. Rev. B **33**, 2370 (1986).
[6] P. J. Durham, C. F. Hague, J.-M. Mariot, and W. M. Temmerman, J. Phys. (Paris) Colloq. **48**, C9-1059 (1987).
[7] B. Ginatempo, G. Y. Guo, W. M. Temmerman, J. B. Staunton, and P. J. Durham, Phys. Rev. **42**, 2761 (1990).
[8] D. A. Papaconstantopoulos, A. Gonis, and P. M. Laufer, Phys. Rev. B **40**, 12 196 (1989).
[9] N. Stefanou, R. Zeller, and P. H. Dederichs, Solid State Commun. **62**, 735 (1987); N. Stefanou, P. J. Braspenning, R. Zeller, and P. H. Dederichs, Phys. Rev. B **36**, 6372 (1987).
[10] J. Kudrnovsky and V. Drchal, Solid State Commun. **70**, 577 (1989); Phys. Rev. B **41**, 7515 (1990).
[11] J. Masek and J. Kudrnovsky, Solid State Commun. **58**, 67 (1986).
[12] J. Hedman, M. Klasson, R. Nilsson, C. Nordling, Phys. Scr. **4**, 195 (1971).
[13] S. Hüfner, G. K. Wertheim, and J. H. Wernick, Solid State Commun. **17**, 1585 (1975).
[14] N. Mårtensson, R. Nyholm, H. Calén, J. Hedman, and B. Johansson, Phys. Rev. B **24**, 1725 (1981).
[15] D. van der Marel, J. A. Jullianus, and G. A. Sawatzky, Phys. Rev. B **32**, 6331 (1985).
[16] H. Wright, P. Weightman, P. T. Andrews, W. Folkerts, C. F. J. Flipse, G. A. Sawatzky, D. Norman, and H. Padmore, Phys. Rev. B **35**, 519 (1987).
[17] M. Davies and P. Weightman, J. Phys. C **17**, L1015 (1984).
[18] The model discussed here is similar to that deduced for 3d impurities in a cubic host crystal discussed by A. Zunger in *Solid State Physics*, edited by H. Ehrenreich and D. Turnbull (Academic, New York, 1986), Vol. 39, p. 275.
[19] R. Magri, S.-H. Wei, A. Zunger, Phys. Rev. B **42** 11 388 (1990).
[20] A. Zunger, S.-H. Wei, L. G. Ferreira, and J. E. Bernard, Phys. Rev. Lett. **65**, 353 (1990).
[21] S.-H. Wei, L. G. Ferreira, J. E. Bernard, and A. Zunger, Phys. Rev. B **42**, 9622 (1990); S. H. Wei and A. Zunger, *ibid.* **43**, 1662 (1991); R. Magri, S. Froyen, and A. Zunger, Phys. Rev. B (to be published).
[22] Z. W. Lu, S.-H. Wei, and A. Zunger (unpublished).
[23] S.-H. Wei and H. Krakauer, Phys. Rev. Lett. **55**, 1200 (1985), and references therein.
[24] G. Lehman and M. Taut, Phys. Status Solidi **54**, 469 (1976).
[25] D. M. Wood and A. Zunger, Phys. Rev. B **40**, 4062 (1989).
[26] R. Yu, D. Singh, and H. Krakauer, Phys. Rev. B **43**, 6411 (1991).
[27] P. Weightman, H. Wright, S. D. Waddington, D. van der Marel, G. A. Sawatzky, G. P. Diakun, and D. Norman, Phys. Rev. **36**, 9098 (1987).